Poly(ethylene glycol)-Mediated Synthesis of Hollow ZnS Microspheres

Yuanyuan Luo, Guotao Duan, Min Ye, Yunxia Zhang, and Guanghai Li*

Key Laboratory of Materials Physics, Anhui Key Laboratory of Nanomaterials and Nanotechnology, Institute of Solid State Physics, Chinese Academy of Sciences, Hefei 230031, People's Republic of China

Received: July 30, 2007; In Final Form: October 31, 2007

Hollow ZnS microspheres composed of nanoparticles have been successfully synthesized by a facile poly(ethylene glycol) (PEG) mediated hydrothermal route. The size of the hollow ZnS microspheres could be adjusted easily by controlling the chain length of PEG. The formation of these hollow microspheres is attributed to the oriented aggregation of ZnS nanorods around a polymer−Zn^{2+} complex spherical framework structure. Different Raman and photoluminescence characters have been observed for the hollow ZnS microspheres with and without PEG. The hollow ZnS microspheres will find potential application in optical and biological devices.

1. Introduction

In recent years, considerable efforts have been dedicated to the synthesis of the porous materials, particularly the hollow structures not only due to their low density, large surface area, and surface permeability but also due to their potential applications in the fields, such as the controllable drug-delivery carriers, lightweight filler, catalyst, photonic crystal, size-selective adsorbent, surface functionalizing, energy storage, and energy conversion.[1−7] The effective control of the internal volume of the hollow structures is essential and a great challenge when used as drug delivery, size-selective adsorbent, and catalysis.[8] Different methods have been used to prepare the hollow structural materials, such as template synthesis,[9−14] Ostwald ripening,[15] emulsion synthesis,[16] "Kirkendall effect",[17] and self-assemble method.[18]

As an important II−VI compound semiconductor, ZnS, with wide band gap energy of 3.6 eV at room temperature, has attracted much attention because of their unique properties and potential applications in ultraviolet light emitting diodes, electroluminescence, photocatalysis, and other optoelectronic devices.[19,20] Because of the high index of refraction and high optical transmission, ZnS is also an attractive candidate for applications in dye materials devices, IR windows, and novel photonic devices operating from visible to near-IR region.[21,22] ZnS nanostructures with the morphologies of nanowires,[23] nanorods,[24,25] nanoribbons,[26] nanobelts,[27] nanotubes,[28] and nanocombs[29] have been reported in the literature; nevertheless, only a few reports are about the hollow ZnS spheres. The ZnS nanospheres with the size of 90−158 nm have been fabricated by controlling the initial concentration of thioacetamide and the molar ratio between thioacetamide and $Zn(NO_3)_2$.[30] The hollow ZnS nanospheres with the size in nanometer scale have been synthesized in aqueous solutions of a triblock copolymer[31] or with the aid of thiocarbamide.[32] The size of the hollow ZnS spheres reported up to now is only on the nanometer scale and can be tuned in a narrow range.

In this paper, we demonstrate a simple one-step hydrothermal synthesis of hollow ZnS microspheres with aid of PEG and the size-related optical properties.

* To whom correspondence should be addressed. E-mail address: ghli@issp.ac.cn. Fax: +86-551-5591434. Tel: +86-551-5591437.

2. Experimental Section

All the reagents of analytical grade were used without further purification. In a typical preparation, 1 g of $Zn(NO_3)_2 \cdot xH_2O$, 0.6 g of PEG (PEG-4000), and 0.4 g of thioacetamide (TAA) were dissolved in 50 mL of distilled water in a flask, and then the mixture was stirred with a magnetic stirrer for 10 min before being transferred to a Teflon-lined autoclave. The autoclave was kept at 200 °C for 10 h and then cooled to room temperature naturally. The precipitates were collected, washed with distilled water and absolute ethanol several times, and dried at 60 °C in vacuum.

Power X-ray diffraction (XRD) analyses were made on the Philips X'Pert using Cu Kα line. An X-ray photoelectron spectrum (XPS) was recorded on a VG ESCALAB Mark II X-ray photoelectron spectroscope. Energy dispersive X-ray (EDX) analysis was obtained on a Sirion 200 scanning electron microscope. The morphology and microstructure were examined using field emission scanning electron microscopy (FESEM, Sirion 200), transmission electron microscopy (TEM, H-800), and high-resolution transmission electron microscopy (HRTEM, JEOL-2010). Raman and photoluminescence (PL) spectra were measured using a LABRAM-HR Micro-Raman spectrometer (Jobin-Yvon) excited with a 325-nm He−Cd laser.

3. Results and Discussion

The XRD patterns of the as-prepared products with and without PEG are shown in Figure 1. One can see that all the diffraction peaks of the products with and without PEG can be indexed to the blende-structured ZnS (JCPDF card 80-0020), and the fairly strong peak intensity shows a well crystallization structure. According to Bragg's formula, the length of the crystalline domain along the (111) direction for the as-prepared productrs with PEG-4000 is evaluated at 0.31 nm. Figure 2 shows the XPS profile of the as-prepared products with PEG-4000, the S 2p peak, and the shoulder peak is identified as S^{2-}, and no elemental S was detected.[27] The quantitative analysis shows the atomic content of S in ZnS is about 45.14%, indicating the excessive Zn atoms in the sample.

Figure 3 shows the typical FESEM images of the as-prepared products with PEG-4000. A spherelike structure with average size of 4.5 μm can be clearly seen in Figure 3a. The micro-

10.1021/jp076047p CCC: $40.75
Published on Web 01/29/2008

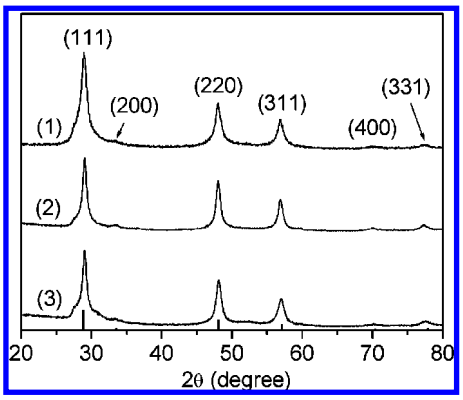

Figure 1. XRD patterns of the as-prepared products with (1) PEG-4000, (2) PEG-800, and (3) without PEG and that from the JCPDS card 80-0020.

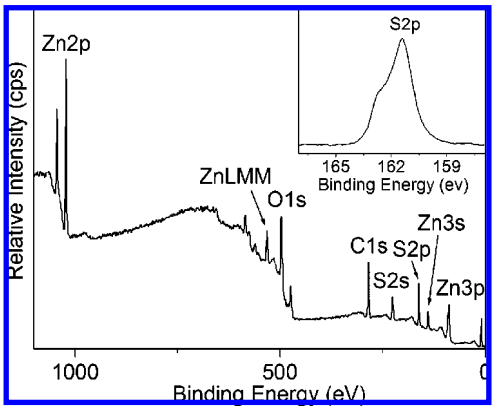

Figure 2. (a) XPS survey and (b) S (2p) profile of as-prepared product with PEG-4000.

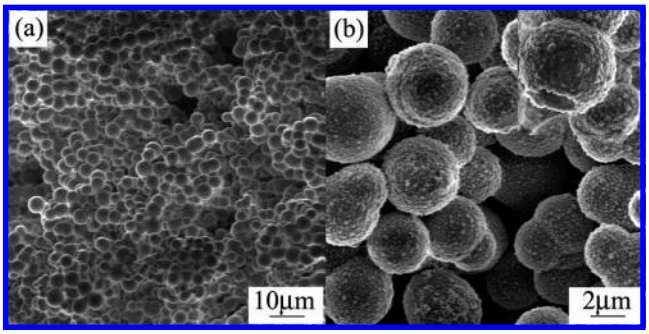

Figure 3. FESEM images of hollow ZnS microspheres with PEG-4000 at different magnifications.

spheres have a rough surface and are composed of nanoparticles with the size of several tens of nanometer in diameter, as shown in Figure 3b. The hollow structure of the microspheres can be clearly seen in the inset in Figure 3b, where the partly broken microsphere clearly shows the hollow feature. The ordered arrangement of the nanoparticles on the edge of the broken microsphere also can be seen. The average shell thickness of the microsphere is about 240 nm. The FESEM image at high magnification further reveals that the nanoparticles have a rodlike morphology with about several tens of nanometers in diameter and 240 nm in length. It is noteworthy that after ultrasonic dispersion for over 40 min only a few microspheres are broken demonstrating that the microspheres are very hard and stable.

Figure 4 shows the TEM images of a broken hollow ZnS sphere with PEG-4000. The hollow structure cannot be seen due to the large shell thickness of the hollow microsphere. An

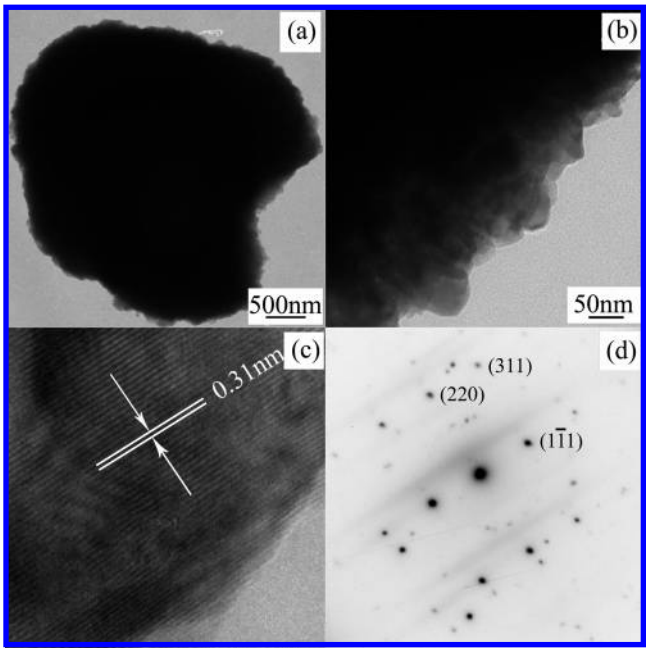

Figure 4. TEM images of (a) a single hollow microsphere with PEG-4000 and (b) the corresponding broken edge region, (c) HRTEM image of the tip region of a nanorod, and (d) the corresponding SAED.

ordered arrangement of the ZnS nanorods at the broken part of the microsphere can be clearly seen (Figure 4b). The HRTEM image of the tip region of a single nanorod (Figure 4c) shows that the fringe spacing is about 0.31 nm, corresponding to the (1$\bar{1}$1) crystal planes of the zinc blende ZnS, which is in accordance with XRD result. The corresponding selected area electron diffraction (SAED) pattern suggests that the nanorod is single crystalline, although there are some additional diffraction spots due to the large diameter of the electron beam. The results indicate that the hollow ZnS microspheres with PEG-4000 are composed of many single crystalline nanorods.

It was found that the size of the hollow ZnS microspheres strongly depends on the chain length of PEG used. The microspheres with a size of about 0.2 μm were obtained without PEG reagent, as shown in Figure 5a, in which the nanoparticles with about several tens of nanometers in size assemble into a loose hollow nanospherical aggregate. When the PEG-800 reagent was used the microspheres with the average size of about 2 μm were formed. The size of the hollow sphere increases to about 4 μm with PEG-2000 (Figure 5c) and further increases to 5 μm with PEG-6000 (Figure 5d). The inset in Figure 5d shows a portion of a broken hollow sphere, in which the hollow structure can be clearly seen. The ZnS nanorod composed of the sphere has an average diameter of about 105 nm and length of about 250 nm. These results demonstrate that the size of the hollow ZnS microspheres is controllable and tunable by changing the PEG chain length.

Figure 6 shows the TEM images of the hollow ZnS spheres without PEG, in which the hollow structure can be clearly seen. The shell of the hollow ZnS spheres consists of an ordered arrangement of the nanorods with an average diameter of about 20 nm and the length of about 50 nm.

Without the PEG, the H_2S from the decomposition of the thioacetamide acts as the nucleation center, and ZnS nanoparticles can nucleate around the H_2S bubbles and then grow in size and finally form hollow ZnS microspheres. When the PEG was added in the $Zn(NO_3)_2$ solution, the metal ions can be easily absorbed on the surface of nonionic surfactant PEG due to strong interactions between activated oxygen in PEG molecular chains

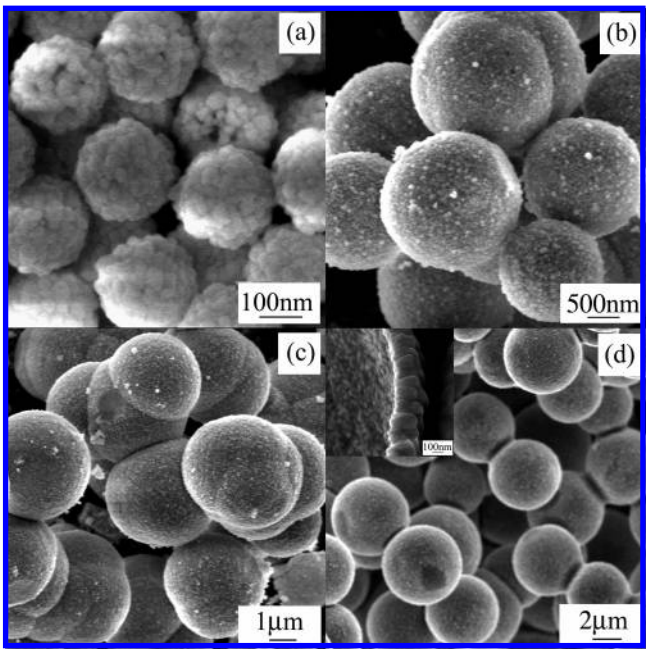

Figure 5. FESEM images of hollow ZnS microspheres (a) without PEG and with (b) PEG-800, (c) PEG-2000, and (d) PEG-6000. The inset in part d is a portion of a broken microsphere.

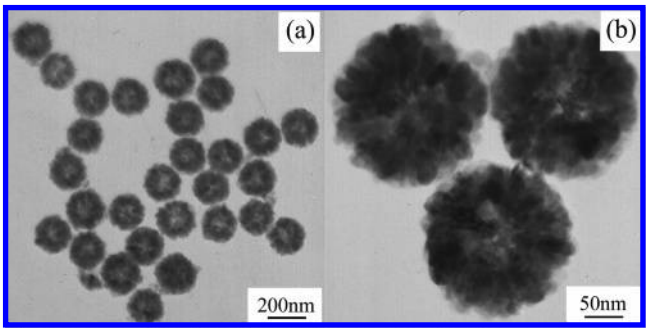

Figure 6. TEM images of the hollow ZnS spheres without PEG at different magnifications.

and metal ions. Because of the long chain structure and flexibility of PEG, the Zn^{2+}−PEG complex can form the framework structure of polymer−Zn^{2+} complex spherical aggregates in water due to the hydrogen-bonding effect. The Zn^{2+} ion-covered complex spherical aggregates are thus formed and provide nucleation centers for the formation of the ZnS nanorods. When the concentration of thioacetamide in the above solution is high enough, more H_2S can be decomposed from the thioacetamide, and many S^{2-} ions are released, the ZnS nanorods then nucleate, oriented grow up, and mineralize on the surface of the Zn^{2+} ion-covered aggregates. Finally, the hollow ZnS microspheres composed of the ZnS nanorods are formed. This formation mechanism is schematically illustrated in Figure 7, which is similar to the formation process of ZnS and PbS hollow spheres reported previously.[33−34] The formation process of the ZnS nanoparticles could be described by the follows reactions

$$CH_3CSNH_2 + H_2O \rightarrow CH_3CONH_2 + H_2S \quad (1)$$

$$H_2S \rightarrow H^+ + HS^- \rightarrow 2\,H^+ + S^{2-} \quad (2)$$

$$Zn^{2+} + S^{2-} \rightarrow ZnS \quad (3)$$

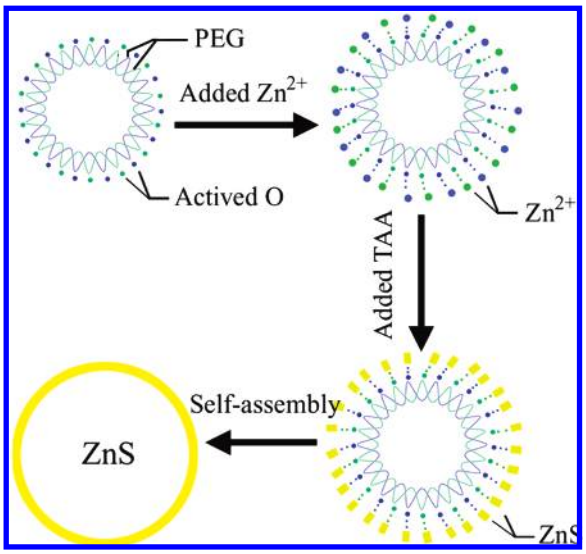

Figure 7. Schematic illustration of the formation mechanism of the hollow ZnS microspheres with PEG.

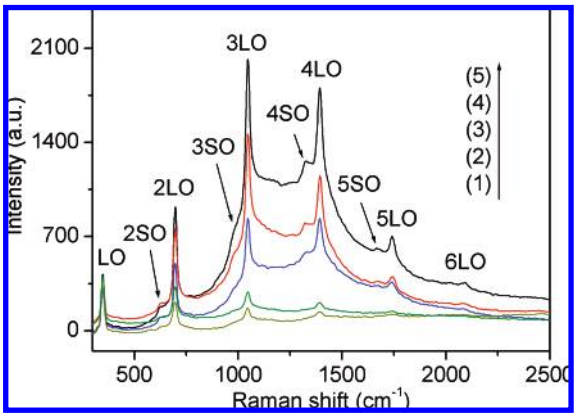

Figure 8. Raman spectra of hollow ZnS microspheres (1) without PEG and with (2) PEG-800, (3) PEG-2000, (4) PEG-4000, and (5) PEG-6000.

Without the PEG reagent, hollow ZnS microspheres are 0.22 μm in size due to a smaller nucleation center around the H_2S bubbles. While with PEG, the longer the chain of the PEG reagent the bigger the framework structure of polymer−Zn^{2+} complex spherical aggregates and thus the bigger the hollow ZnS microspheres. The size of hollow ZnS microspheres formed oriented around the framework structure of the polymer−Zn^{2+} complex spherical aggregates gradually increases with increasing the chain length of the PEG reagent.

The Raman spectra of the microspheres with different PEG chain length are shown in Figure 8. The laser exciting power intensity is $I_0/10$, in which the full excitation power intensity (I_0) is about 2 Kw·cm^{-2}. Six resonant Raman peaks situated at 348.1, 696.5, 1045.1, 1393.2, 1740.3, and 2090.0 cm^{-1} and designated as the first-order longitudinal optical (1LO), second-order (2LO), third-order (3LO), fourth-order (4LO), fifth-order (5LO), and sixth-order (6LO) optical phonon mode, respectively,[35] can be observed for the microspheres with PEG-6000. The excitation energy is close to the photon-scattering energy of the third- and the fourth-order LO phonons, and thus the photon scattering by the third and the fourth order LO phonons is resonant with the excitons, and intensities of these two LO peaks are stronger than that of the rest of LO peaks. The other four abnormal weaker peaks marked SO in the Raman spectra

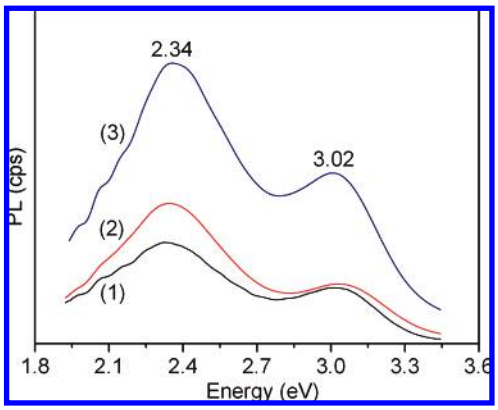

Figure 9. PL spectra of hollow ZnS microspheres (1) with PEG-800, (2) with PEG-4000, and (3) without PEG.

are considered correlate to the surface optical (SO) phonon scattering. The energy of the SO phonon mode in multiphonon scattering equals 332 cm^{-1}, which is between the LO phonon energy and the TO phonon energy.[36] The detailed discussion about the SO phonon mode can be found elsewhere.[37] The intensities of the basic fluorescence band and the LO and SO phonon peaks gradually became weak, and some of the SO phonon peaks finally disappeared with the decrease in the PEG chain length, which might be due to the size effect of the nanorods. The existence of the multiple resonant Raman bands at room temperature indicates that the hollow ZnS microspheres have a good optical quality,[38] while the appearance of the higher-order surface optical (SO) phonon mode predicts that there are defects on the surface of the hollow ZnS microspheres.[39]

The PL properties of the hollow ZnS microspheres synthesized with and without PEG are shown in Figure 9, in which two PL peaks situated, respectively, at about 3.02 and 2.34 eV can be clearly seen. No obvious difference of the PL feature can be observed for the microspheres with different PEG chain lengths. The sulfur vacancies on the surface of the hollow ZnS microspheres could be responsible for the weak emission at 3.02 eV,[24,40,41] which is in agreement with the result of Raman spectra analysis. The strong emission at 2.34 eV could be assigned to the recombination of electrons from the energy level of sulfur vacancies to holes on the energy level of zinc vacancies.[42−45]

4. Conclusion

The hollow ZnS microspheres have been synthesized by hydrothermal method with the aid of PEG. The hollow ZnS microspheres are composed of ZnS nanorods. The formation of these hollow spheres is attributed to the oriented aggregation of ZnS nanorods around polymer−Zn^{2+} complex spherical framework structure. It was found the size of the hollow ZnS microspheres could be controlled by the PEG chain length. A strong resonant Raman scattering spectrum with high-order longitudinal optical mode and weak high-order surface optical mode has been observed. There are two PL peaks for the hollow ZnS microspheres with PEG and without PEG. It is believed that such hollow ZnS microspheres with tunable size will find potential applications in sensor, optical and biological devices.

Acknowledgment. This work was supported by the National Natural Science Foundation of China (No. 10674137) and National Basic Research Program of China (No. 2007CB936601).

References and Notes

(1) Caruso, F.; Caruso, R. A.; Möhwald, H. *Science* **1998**, *282*, 1111.
(2) Yang, H. G.; Zeng, H. C. *Angew. Chem.* **2004**, *116*, 6056.
(3) Duan, G. T.; Cai, W. P.; Luo, Y. Y.; Li, Z. G.; Lei, Y. *J. Phys. Chem. B* **2006**, *110*, 15729.
(4) Fang, X. S.; Ye, C. H.; Zhang, L. D.; Wang, Y. H.; Wu, Y. C. *Adv. Funct. Mater*. **2005**, *15*, 63.
(5) Shchukin, D. G.; Patel, A. A.; Sukhorukov, G. B.; Lvov, Y. M. *J. Am. Chem. Soc.* **2004**, *126*, 3374.
(6) Zhang, Y. X.; Li, G. H.; Wu, Y. C.; Luo, Y. Y.; Zhang, L. D. *J. Phys. Chem. B* **2005**, *109*, 5478.
(7) Duan, G. T.; Cai, W. P.; Luo, Y. Y.; Sun, F. Q. *Adv. Funct. Mater.* **2007**, *17*, 644.
(8) Zhao, Q. H.; Han, B. S.; Wang, Z. H.; Gao, C. Y.; Peng, C. H.; Shen, J. C. *Nanomedicine* **2007**, *3*, 63.
(9) Schwartzberg, A. M.; Olson, T. Y.; Talley, C. E.; Zhang, J. Z. *J. Phys. Chem. B* **2006**, 110, 19935. Liang, H. P.; Wan, L. J.; Bai, C. L.; Jiang, L. *J. Phys. Chem. B* **2005**, *109*, 7795.
(10) Davis, S. A.; Burkett, S. L.; Mendelson, N. H.; Mann, S. *Nature* **1997**, *385*, 420.
(11) Li, Y.; Huang, X. J.; Heo, S. H.; Li, C. C.; Choi, Y. K.; Cai, W. P.; Cho, S. O. *Langmuir* **2007**, *23*, 2169. Cölfen, H.; Antonietti, M. *Langmuir* **1998**, *14*, 582.
(12) Sun, X.; Li, Y. *Angew. Chem., Int. Ed.* **2004**, *43*, 3827.
(13) Im, S. H.; Jeong, U.; Xia, Y. *Nat. Mater.* **2005**, *4*, 671.
(14) Xu, X.; Asher, S. A. *J. Am. Chem. Soc.* **2004**, *126*, 7940.
(15) Yang, H. G.; Zeng, H. C. *J. Phys. Chem. B* **2004**, *108*, 3492.
(16) Imhof, A.; Pine, J. *Nature* **1997**, *389*, 948.
(17) Liu, B.; Zeng, H. C. *J. Am. Chem. Soc.* **2004**, *126*, 16744.
(18) Park, S.; Lim, J. H.; Chung, S. W.; Mirkin, C. A. *Science* **2004**, *303*, 348.
(19) Fang, X. S.; Zhang, L. D. *J. Mater. Sci. Technol.* **2006**, *22*, 721. Li, Y. Q.; Zapien, J. A.; Shan, Y. Y.; Liu, Y. K.; Lee, S. T. *Appl. Phys. Lett.* **2006**, *88*, 013115.
(20) Moore, D.; Wang, Z. L. *J. Mater. Chem.* **2006**, *16*, 3898. Yu, S. H.; Yoshimura, M. *Adv. Mater.* **2002**, *14*, 296.
(21) Bredol, M.; Merikhi, J. J. *J. Mater. Sci.* **1998**, *33*, 471.
(22) Yamada, Y.; Yoshimura, K.; Fujita, S.; Taguchi, T. *Appl. Phys. Lett.* **1997**, *70*, 1429.
(23) Dorothy Duo Duo Ma; Lee, S. T. *Nano Lett.* **2006**, *6*, 926.
(24) Liang, C. H.; Shimizu, Y.; Sasaki, T,; Umehara, H.; Koshizaki, N. *J. Phys. Chem. B* **2004**, *108*, 9728.
(25) Yu, J. H.; Joo, J.; Park, H. M.; Baik, Sung-Il. Kim, Y. W.; Kim, S. C.; Hyeon, T. *J. Am. Chem. Soc.* **2005**, *127*, 5662.
(26) Fan, X.; Meng, X. M.; Zhang, X. H.; Shi, W. S.; Zhang, W. J.; Zapien, J. A.; Lee, C. S.; Lee, S. T. *Angew. Chem., Int. Ed.* **2006**, *45*, 2568.
(27) Ye, C. H.; Fang, X. S.; Li, G. H.; Zhang, L. D. *Appl. Phys. Lett.* **2004**, *85*, 3035.
(28) Yin, L. W.; Bando, Y.; Zhan, J. H.; Li, M. S.; Golberg, D. *Adv. Mater.* **2005**, *17*, 1972.
(29) Ma, C.; Moore, D.; Li, J.; Wang, Z. L. *Adv. Mater*. **2003**, *15*, 228.
(30) Wolosiuk, A.; Armagan, O.; Braun, P. V. *J. Am. Chem. Soc.* **2005**, *127*, 16356.
(31) Ma, Y. R.; Qi, L. M.; Ma, J. M.; Cheng, H. M. *Langmuir* **2003**, *19*, 4040.
(32) Liu, H. J.; Ni, Y. H.; Han, M.; Liu, Q.; Xu, Z.; Hong, J. M.; Ma, X. *Nanotechnology* **2005**, *16*, 2908.
(33) Gu, F.; Li, C. Z.; Wang, S. F.; Lü, M. K. *Langmuir* **2006**, *22*, 1329; Wang, S. F.; Gu, F.; Lü, M. K. *Langmuir* **2006**, *22*, 398.
(34) Liu, H. J.; Ni, Y. H.; Han, M.; Liu, Q.; Xu, Z.; Hong, J. M.; Ma, X. *Nanotechnology* **2005**, *16*, 2908. Zhang, H.; Zhang, S. Y.; Pan, S.; Li, G. P.; Hou, J. G. *Nanotechnology* **2004**, *15*, 945.
(35) Nilsen, W. G. *Phys. Rev.* **1969**, *182*, 838.
(36) Xiong, Q. H.; Wang, J. G.; Reese, O.; Lew Yan Voon, L. C. Eklund, P. C. *Nano Lett.* **2004**, *4*, 1991.
(37) Luo, Y. Y.; Duan, G. T.; Li, G. H. *Appl. Phys. Lett.* **2007**, *90*, 201911.
(38) Kumar, B.; Gong, H.; Chow, S. Y.; Tripathy, S.; Hua, Y. N. *Appl. Phys. Lett*. **2006**, *89*, 071922.
(39) Ursaki, V. V.; Tiginyanu, I. M.; Zalamai, V. V.; Rusu, E. V.; Emelchenko, G. A.; Masalov, V. M.; Samarov, E. N. *Phys. Rev. B.* **2004**, *70*, 155204.
(40) Jiang, X.; Xie, Y.; Lu, J.; Zhu, L.; He, W.; Qian, Y. *Chem. Mater.* **2001**, *13*, 1213.
(41) Ishizumi, A.; White, C. W.; Kanemitsu, Y. *Appl. Phys. Lett.* **2004**, *84*, 2398.
(42) Biswas, S.; Kar, S.; Chaudhuri, S. *J. Phys. Chem. B* **2005**, *109*, 17526.
(43) Falcony, C.; Garcia, M.; Ortiz, A.; Alonso, J. C. *J. Appl. Phys.* **1992**, *72*, 1525.
(44) Samelson, H.; Lempicki, A. *Phys. Rev.* **1962**, *125*, 901.
(45) Lu, H. Y.; Chu, S. Y.; Tan, S. S. *J. Cryst. Growth* **2004**, *269*, 385.